Biochimica et Biophysica Acta 1848 (2015) 731–741

Contents lists available at ScienceDirect

Biochimica et Biophysica Acta

journal homepage: www.elsevier.com/locate/bbamem

Pharmacological and molecular studies on the interaction of varenicline with different nicotinic acetylcholine receptor subtypes. Potential mechanism underlying partial agonism at human α4β2 and α3β4 subtypes

Hugo R. Arias [a,*], Dominik Feuerbach [b], Katarzyna Targowska-Duda [c], Agnieszka A. Kaczor [d], Antti Poso [e], Krzysztof Jozwiak [c]

[a] Department of Medical Education, California Northstate University College of Medicine, Elk Grove, CA, USA
[b] Neuroscience Research, Novartis Institutes for Biomedical Research, Basel, Switzerland
[c] Department of Chemistry, Laboratory of Medicinal Chemistry and Neuroengineering, Medical University of Lublin, Lublin, Poland
[d] Department of Synthesis and Chemical Technology of Pharmaceutical Substances with Computer Modeling Lab, Medical University of Lublin, Lublin, Poland
[e] School of Pharmacy, University of Eastern Finland, Kuopio, Finland

ARTICLE INFO

Article history:
Received 12 August 2014
Received in revised form 29 October 2014
Accepted 6 November 2014
Available online 2 December 2014

Keywords:
Varenicline
Nicotinic acetylcholine receptors
Partial agonist
Full agonist
Molecular modeling

ABSTRACT

To determine the structural components underlying differences in affinity, potency, and selectivity of varenicline for several human (h) nicotinic acetylcholine receptors (nAChRs), functional and structural experiments were performed. The Ca^{2+} influx results established that: (a) varenicline activates (μM range) nAChR subtypes with the following rank sequence: hα7 > hα4β4 > hα4β2 > hα3β4 >>> hα1β1γδ; (b) varenicline binds to nAChR subtypes with the following affinity order (nM range): hα4β2 ~ hα4β4 > hα3β4 > hα7 >>> *Torpedo* α1β1γδ. The molecular docking results indicating that more hydrogen bond interactions are apparent for α4-containing nAChRs in comparison to other nAChRs may explain the observed higher affinity; and that (c) varenicline is a full agonist at hα7 (101%) and hα4β4 (93%), and a partial agonist at hα4β2 (20%) and hα3β4 (45%), relative to (±)-epibatidine. The allosteric sites found at the extracellular domain (EXD) of hα3β4 and hα4β2 nAChRs could explain the partial agonistic activity of varenicline on these nAChR subtypes. Molecular dynamics simulations show that the interaction of varenicline to each allosteric site decreases the capping of Loop C at the hα4β2 nAChR, suggesting that these allosteric interactions limit the initial step in the gating process. In conclusion, we propose that in addition to hα4β2 nAChRs, hα4β4 nAChRs can be considered as potential targets for the clinical activity of varenicline, and that the allosteric interactions at the hα3β4- and hα4β2-EXDs are alternative mechanisms underlying partial agonism at these nAChRs.

1. Introduction

The addictive properties of nicotine (the active alkaloid involved in smoking addiction) as well as the activity of varenicline (Chantix®, Champix®) for smoking cessation therapy [1] are primarily mediated by their interactions with nicotinic acetylcholine receptors (nAChRs). The interaction of nicotine with α4β2 nAChRs in the mesocorticolimbic system, the so-called "brain reward system", increases the synaptic levels of dopamine, which in turn produces the pleasurable effects mediated by nicotine [2–4]. There is a large amount of experimental evidence supporting an important role of α4β2 nAChRs in the mechanism of nicotine addiction. For example, animal studies show that agonists specific for α4β2 nAChRs produce similar discriminative stimulus as nicotine [5], and knockout animal results indicates that the β2 subunit is necessary for the reinforcing [6] and discriminative [7] properties

Abbreviations: nAChR, nicotinic acetylcholine receptor; [^{3}H]MLA, [^{3}H]methyllycaconitine; [^{3}H]TCP, piperidyl-3, 4-^{3}H(*N*)]-(*N*-(1-(2 thienyl)cyclohexyl)-3, 4-piperidine; α-BTx, α-bungarotoxin; Varenicline, 7,8,9,10-tetrahydro-6,10-methano-6*H*-azepino[4,5-*g*]quinoxaline; RT, room temperature; BS, binding saline; A, allosteric; EXD, extracellular domain, ORT, orthosteric; A, allosteric; TMD, transmembrane domain, K_i, inhibition constant; K_d, dissociation constant; IC_{50}, ligand concentration that produces 50% inhibition (of binding or of agonist activation); EC_{50}, agonist concentration that produces 50% nAChR activation; n_H, Hill coefficient; MD, molecular dynamics; NVT, constant number of particles, volume, and temperature; NPT, constant number of particles, pressure, and temperature; RMSD, root mean square deviation; DMEM, Dulbecco's Modified Eagle Medium; FBS, fetal bovine serum; FLIPR, fluorescent imaging plate reader

* Corresponding author at: Department of Medical Education, California Northstate University College of Medicine, 9700 W. Taron Dr., Elk Grove, CA 95757, USA. Tel.: +1 916 686 7304; fax: +1 916 686 7310.
E-mail address: hugo.arias@cnsu.edu (H.R. Arias).

http://dx.doi.org/10.1016/j.bbamem.2014.11.003
0005-2736/

of nicotine and for nicotine-induced dopamine release [8]. Nevertheless, other nAChR subtypes (i.e., α7, α3β4, and α6β2-containing nAChRs) are also involved in the mechanism of nicotine addiction [2,3].

Pharmacologically, varenicline behaves as a partial agonist of α4β2 nAChRs and a full agonist of α7 nAChRs [9–12]. Through its intrinsic partial activation of α4β2 nAChRs, varenicline elicits a moderate and sustained increase of dopamine levels in the brain reward system, which would elevate low dopamine levels observed during smoking cessation attempts [4,11–14]. In addition, varenicline competitively inhibits nicotine binding to α4β2 nAChRs, preventing nicotine-induced dopaminergic activation. This dual effect ultimately decreases craving, withdrawal symptoms, smoking satisfaction and reward. Studies using β2-subunit knockout animals and animals where the β2 subunit has been re-expressed indicate that β2-containing nAChRs are involved in the dopaminergic effects mediated by varenicline [15]. Although there is a good idea of how varenicline acts clinically, we still do not have a complete understanding of the structural and functional aspects underlying its receptor selectivity, specifically regarding the α4β4 nAChR. α4 and β4 subunits, potentially forming α4β4-containing nAChRs, are also expressed in several brain regions implicated in drug addiction, including basal ganglia, cerebellum, midbrain, ventral tegmental area, hippocampus, and cortex [16,17]. To have a more comprehensive idea of the interaction of varenicline with different nAChR subtypes, we decided to determine which structural components are important for the different binding affinities, agonistic and antagonistic potencies, and receptor selectivity of varenicline for several nAChR subtypes including, the human (h) α4β2, hα4β4, hα3β4, hα7, *Torpedo* and hα1β1γδ nAChRs. In this study we applied structural and functional approaches including radioligand binding assays, Ca^{2+} influx-induced fluorescence detections, as well as homology modeling, molecular docking, and molecular dynamics studies.

2. Materials and methods

2.1. Materials

[^{3}H]Epibatidine (45.1 Ci/mmol), [^{3}H]cytisine (34.1 Ci/mmol), [piperidyl-3,4-^{3}H(*N*)]-(*N*-(1-(2 thienyl)cyclohexyl)-3,4-piperidine) ([^{3}H]TCP; 45.0 Ci/mmol), and [^{3}H]imipramine (47.5 Ci/mmol) were obtained from PerkinElmer Life Sciences Products, Inc. (Boston, MA, USA). [^{3}H]Methyllycaconitine (100 Ci/mmol) was purchased from American Radiolabeled Chemicals Inc. (Saint Louis, MO, USA). The radioligands were stored at −20 °C. Methyllycaconitine citrate, carbamylcholine dihydrochloride, imipramine hydrochloride, and polyethylenimine were purchased from Sigma Chemical Co. (St. Louis, MO, USA). (±)-Epibatidine hydrochloride was obtained from Tocris Bioscience (Ellisville, Missouri, USA). Fetal bovine serum (FBS) and trypsin/EDTA were purchased form Gibco BRL (Paisley, UK). Ham's F-12 Nutrient Mixture was obtained from Invitrogen (Paisley, UK). Varenicline hydrochloride and phencyclidine hydrochloride (PCP) were obtained through the National Institute on Drug Abuse (NIDA) (NIH, Baltimore, USA). Salts were of analytical grade.

2.2. Ca^{2+} influx measurements in cells containing different nAChR subtype

Ca^{2+} influx measurements were performed in GH3-hα7, HEK293-hα4β2, HEK293-hα3β4, and TE671-hα1β1γδ cells incubated at 37 °C as previously described [17–19]. In the particular case of CHO-hα4β4 cells, a density of 5×10^4 per well was used. Under these conditions, the majority of expressed nAChRs has the $(\alpha x)_3(\beta x)_2$ stoichiometry (see [18] and references therein). To determine the agonistic activity, varenicline or (±)-epibatidine was added to the cell plate using the 96-tip pipettor simultaneously to fluorescence recordings for a total length of 3 min. To determine the antagonistic activity, cells were pretreated (5 min) with different concentrations of varenicline before testing the activity of (±)-epibatidine (0.1 μM for neuronal nAChRs, and 1 μM for hα1β1γδ nAChRs).

2.3. Radioligand competition binding experiments

To determine receptor selectivity, the effect of varenicline on [^{3}H]MLA (4.1 nM) binding to hα7 nAChRs, on [^{3}H]epibatidine (4.6 nM) binding to hα3β4 nAChRs, and on [^{3}H]cytisine (9.1 nM) binding to hα4β2, hα4β4, and *Torpedo* nAChRs, respectively, was studied as previously described [19–22]. To determine whether varenicline interacts with the *Torpedo* and hα4β2 nAChR ion channels, additional studies were conducted using [^{3}H]TCP (20 nM) [21] and [^{3}H]imipramine (13 nM) [23]. The effect of varenicline on [^{3}H]cytisine, in the absence (nAChRs are in the resting but activatable state) and presence of 200 μM proadifen [24], and [^{3}H]TCP binding, in the presence of 1 mM CCh (nAChRs are mainly in the desensitized state), was also determined as previously described [21,23]. Nonspecific binding was determined in the presence of 10 μM MLA ([^{3}H]MLA experiments), 1 mM CCh ([^{3}H]cytisine experiments), 0.2 μM (±)-epibatidine ([^{3}H]epibatidine experiments), 100 μM PCP ([^{3}H]TCP experiments), or 100 μM imipramine ([^{3}H]impramine experiments).

After incubation (2 h), nAChR-bound radioligand was separated from free radioligand by a filtration assay [19–23]. The concentration–response data were curve-fitted by nonlinear least squares analysis using the Prism software (GraphPad Software, San Diego, CA). The observed IC_{50} values were transformed into inhibition constant (K_i) values using the Cheng–Prusoff relationship [25]:

$$K_i = IC_{50} \Big/ \left\{1 + \left(\left[\left[{}^3H \right] \text{ligand} \right] \Big/ K_d^{\text{ligand}} \right) \right\} \quad (1)$$

where [[^{3}H]ligand] is the initial concentration of [^{3}H]MLA, [^{3}H]cytisine, or [^{3}H]epibatidine, and K_d^{ligand} is the dissociation constant for [^{3}H]MLA (1.86 nM for the hα7 nAChR [26]), [^{3}H]cytisine (0.1 nM for the hα4β4 nAChR [27], 0.3 nM for the hα4β2 nAChR [28] and 0.45 μM for the desensitized *Torpedo* nAChR [22]), and [^{3}H]epibatidine (89 pM for the hα3β4 AChR [29]). The calculated K_i values were summarized in Table 2.

2.4. Homology models of the hα3β4, hα4β4, hα4β2, and hα7 nAChRs

The crystal structure of the acetylcholine binding protein (AChBP) (PDB 4AFT) [30] was used as a template for the extracellular domain of the human (h)α3β4, hα4β4, hα4β2, and hα7 nAChRs, whereas the *Torpedo* nAChR model (PDB 2BG9) [31] was used as a template for the transmembrane domains (TMD). Water molecules were added to the model according to the AChBP-cytisine structure (PDB 4AFO) [30]. The amino acid sequence of each nAChR subunit (i.e., hα7, hα3, hα4, hβ2, and hβ4) was first aligned with corresponding sequences of the AChBP and *Torpedo* nAChR subunits by using the ClustalW2 server (www.ebi.ac.uk/Tools/msa/clustalw2) [32]. A hundred homology models for each nAChR subtype were generated using Modeller v.9.9 [33], and subsequently assessed by Modeller objective function and Discrete Optimized Protein Energy profiles [34]. The best model of each nAChR subtype was subjected to quality assessments using the Molecular Environment module for Ramachandran plots (http://www.chemcomp.com/software.htm) and the web-based tools of Annolea [35], Verify3D [36], and ProCheck [37].

2.5. Molecular docking

Docking simulations were performed using the same protocol as reported previously [19]. In addition, water molecules were incorporated within the binding pockets. The crystal structure of varenicline, transferred from its crystal model with AChBP, was used for the subsequent step of molecular docking. Molegro Virtual Docker (MVD v 5.0.0,

Molegro ApS Aarhus, Denmark) was used for docking simulations of flexible ligands (i.e., varenicline in the neutral and protonated states) into the rigid nAChR target. The docking space was extended to ensure covering two subunits (i.e., α3/β4, α4/β4, α4/β2, α7/α7, α1/δ, and α1/γ) containing the orthosteric (ORT) site, as well as the extracellular domain (EXD) from each nAChR model for additional allosteric (A) sites. The actual docking simulations were performed using the settings described previously [19,23,38]. The lower energy conformations were selected from each cluster of superposed poses.

2.6. Molecular dynamics simulations

To investigate the stability of varenicline at the suggested docking sites, molecular dynamics (MD) simulations were performed by using Desmond v. 3.0.3.1 [39] and OPLS-2005 force field. Each nAChR-varenicline model was inserted into 1-palmitoyl-2-oleoyl phosphatidylcholine membranes, solvated with water as described previously [40] and ions were added to neutralize the protein charges as described elsewhere [41]. Each nAChR model was first minimized and then subjected to 1-ns MD in NVT (constant number of particles, volume, and temperature) ensemble, followed by 15-ns MD in NPT (constant number of particles, pressure, and temperature) ensemble. Although fixing constrains for backbone atoms were assigned, all side-chain atoms were left free to move during the simulations. The total potential energy of each docked model was calculated using the OPLS-2005 force field according to Bowers et al. [39].

To determine how the binding of varenicline to each allosteric site found at the hα4β2 nAChR modifies the interaction of the ligand at the ORT site, only the EXD was studied. The MD procedure was similar to that described before, although 25-ns MD in NPT ensemble with protein backbone restrains and additional 25-ns MD without restraints was used instead. Four models were simulated, when varenicline is bound to: (1) two ORT sites only (control), (2) two ORT and A1 allosteric sites, (3) two ORT and A2 allosteric sites, and to (4) two ORT and A3 allosteric sites.

3. Results

3.1. Pharmacologic activity of varenicline assessed by Ca^{2+} influx in cells expressing different nAChR subtypes

The agonistic potency of varenicline was first determined by assessing the fluorescence change on each nAChR-expressing cell line after its direct stimulation (Fig. 1). The observed receptor selectivity follows the order (EC_{50}s in μM): hα7 (0.18 ± 0.02) > hα4β4 (0.37 ± 0.08) > hα4β2 (1.30 ± 0.18) > hα3β4 (6.4 ± 1.2) ≫ > hα1β1γδ (>100) (Table 1). Based on the observed efficacy (E_{max}), varenicline is a full agonist of the hα7 (101 ± 8%) and hα4β4 (93 ± 7%) nAChRs, and a partial agonist of the hα4β2 (20 ± 6%) and hα3β4 (45 ± 10%) nAChRs. In general, our results support previous data [10–12,42]. However, this is the first report showing that varenicline behaves as a full agonist of hα4β4 nAChRs. The competitive properties of varenicline

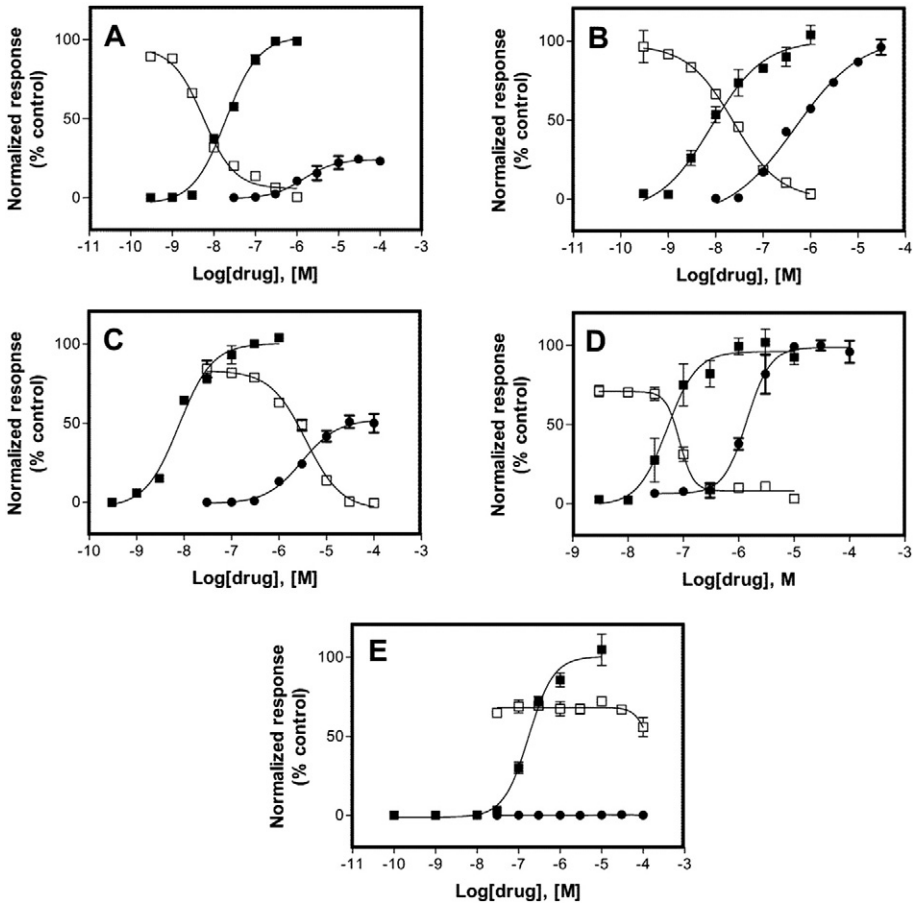

Fig. 1. Functional activity of varenicline on (A) HEK293-hα4β2, (B) CHO-hα4β4, (C) HEK293-hα3β4, (D) GH3-hα7, and (E) TE671-hα1β1γδ cells using Ca^{2+} influx measurements. Increased concentrations of (±)-epibatidine (■) or varenicline (●) enhance intracellular calcium. The competitive effect of varenicline was investigated by pretreating (5 min) the cells with different concentrations of varenicline followed by activation of the receptor with (±)-epibatidine (□). The plots for the agonistic action of varenicline are the combination of 6 (A and D), 4 (B), and 3 (C and E) experiments, respectively. The plots for the antagonistic action of varenicline are the combination of 4 (A), 6 (B), 5 (C), 8 (D), and 3 (E) experiments, respectively. The error bars represent the standard deviation (S.D.). Ligand response was normalized to the maximal (±)-epibatidine response, which was set as 100%. The calculated E_{max}, EC_{50}, IC_{50}, and n_H values are summarized in Table 1.

Table 1
Stimulation and inhibition elicited by varenicline at different nAChR subtypes assessed by Ca^{2+} influx assays.

nAChR subtype	EC_{50} (μM)	E_{max}	n_H[a]	IC_{50} (nM)	n_H[a]
hα4β2	1.30 ± 0.18	20 ± 6	1.51 ± 0.21	2.8 ± 1.2	1.87 ± 0.46
hα4β4	0.37 ± 0.08	93 ± 7	1.15 ± 0.22	26.7 ± 2.4	0.93 ± 0.06
hα3β4	6.4 ± 1.2	45 ± 10	1.80 ± 0.32	2336 ± 762	1.50 ± 0.21
hα7	0.18 ± 0.02	101 ± 8	4.04 ± 0.97	69.0 ± 8.1	3.85 ± 0.59
hα1β1γδ	>100	–	–	>100,000	–

These values were obtained from Fig. 1A–E, respectively.
[a] Hill coefficient.

were also investigated by pre-incubating the nAChR with varenicline before the (±)-epibatidine-induced nAChR activation (Fig. 1). In this regard, the inhibitory (i.e., desensitizing) potency follows the order (IC_{50}s in nM): hα4β2 (2.8 ± 1.2) > hα4β4 (26.7 ± 2.4) > hα7 (69.0 ± 8.1) > hα3β4 (2336 ± 762) ≫ > hα1β1γδ (>100,000).

The observed n_H values are higher than unity, except that for hα4β4 nAChRs (Table 1). This suggests that varenicline activates the nAChRs and antagonizes the agonist-activated nAChRs in a cooperative manner, supporting the existence of more than one binding site on each nAChR, except on hα4β4 nAChRs. This observation is more apparent in the hα7 nAChR, coinciding with the experimental results showing that at least three agonist sites need to be occupied to activate this ion channel [43]. n_H values higher than unity were also found on the hα4β2 nAChR by voltage-clamp measurements [12].

3.2. Radioligand binding experiments

The binding affinity of varenicline for each nAChR subtype was determined by radioligand binding (Fig. 2A–C). The calculated K_i values demonstrate that varenicline binds to the hα4β4 (121 ± 4 pM) and hα4β2 (90 ± 7 pM) nAChRs with practically the same affinity (Table 2). Moreover, varenicline binds to the hα7 (100 ± 7 nM), hα3β4 (13 ± 1 nM), and desensitized *Torpedo* (116 ± 8 μM) nAChRs with ~100–1,000,000-fold lower affinity compared to that for α4-containing nAChRs. Previous studies support our binding affinity results [9,11,12,44]. In a simplistic way, the calculated n_H values suggest that varenicline inhibits radioligand binding in a non-cooperative manner (Table 2). In addition, varenicline enhances [^{3}H]cytisine binding to *Torpedo* nAChRs in the resting but activatable state (i.e., in the absence of proadifen) (Fig. 2D), whereas in the desensitized state (i.e., in the presence of proadifen) it binds to the nAChR agonist sites with very low affinity (Table 2).

To further determine whether varenicline binds to the nAChR channel or not, additional [^{3}H]TCP competition experiments were performed (Fig. 3A). The results indicate that varenicline enhances [^{3}H]TCP binding when the nAChR is in the resting but activatable state (in the absence of CCh), with the same apparent EC_{50} value as that for [^{3}H]cytisine binding enhancement (Table 2). This result suggests that varenicline does not bind to the TCP site when the *Torpedo* nAChR is in the resting (i.e., in the absence of CCh) or desensitized (i.e., in the presence of CCh) state (Fig. 3A). A simple explanation for the result in the resting state is that when varenicline binds to its orthosteric sites at the *Torpedo* nAChR, the receptor becomes desensitized, and thus [^{3}H]TCP binding to the ion channel is enhanced. The [^{3}H]TCP results were corroborated by additional [^{3}H]imipramine competition experiments in the hα4β2 nAChR (Fig. 3B), where an apparent IC_{50} value of ~12 mM (n_H < 0.5) was estimated from these experiments (Table 2). These data support the idea that varenicline inhibits [^{3}H]imipramine binding with extremely low affinity. However, we cannot rule out the possibility that varenicline binds to a luminal site located apart from the TCP/imipramine locus.

3.3. Molecular docking of varenicline with different nAChR subtypes

Varenicline, in the neutral and protonated state, was docked to the EXD from each nAChR subtype (i.e., hα3β4, hα4β4, hα4β2, and hα7). Since varenicline is highly protonated (~100%) at physiological pH [pK_a values of 9.8 ± 0.2 calculated by the ACD/ADME Suite software (Advanced Chemistry Development, Inc., Toronto, Canada)] the different modes of binding are shown only for the protonated state. The docking results indicate that varenicline interacts with ORT and allosteric (A) binding sites (Table 3).

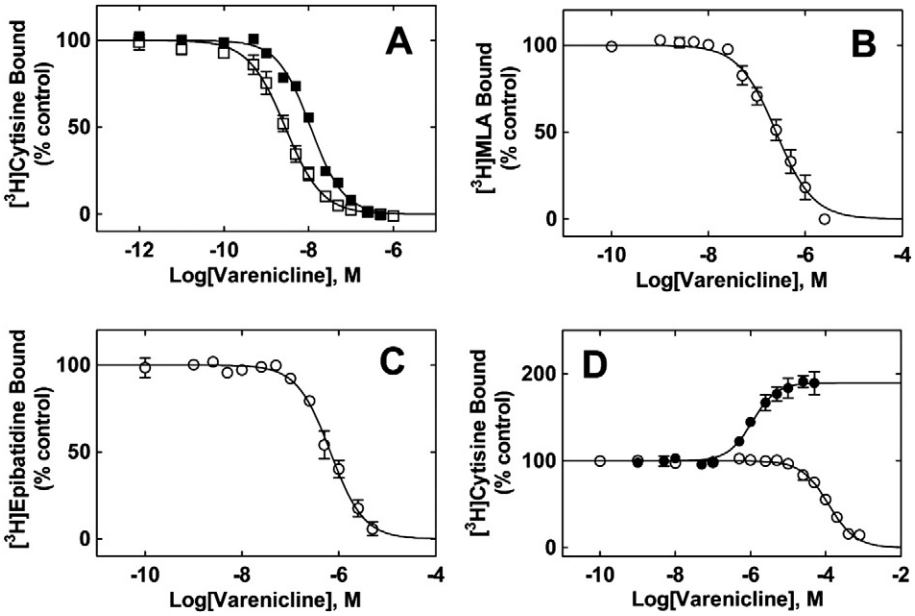

Fig. 2. Varenicline-induced inhibition of (A) [^{3}H]cytisine binding to hα4β4 (■) and hα4β2 (□) nAChRs, (B) [^{3}H]MLA binding to hα7 nAChRs, (C) [^{3}H]epibatidine binding to hα3β4 nAChRs, and of (D) [^{3}H]cytisine binding to *Torpedo* nAChRs in the resting but activatable (●) and desensitized (○) states, respectively. nAChR membranes (1–2 mg/mL) were pre-incubated (30 min) with 9.1 nM [^{3}H]cytisine, 4.6 nM [^{3}H]epibatidine, or 4 nM [^{3}H]MLA, respectively, and then equilibrated (2 h) with increasing concentrations of varenicline. To maintain the *Torpedo* nAChR in the desensitized state, *Torpedo* nAChR membranes were pre-incubated with 200 proadifen (○). Nonspecific binding was determined at 1 mM CCh (A and D), 10 μM MLA (B), and 0.2 μM (±)-epibatidine (C), respectively. Each plot is the combination of 2–3 separated experiments each one performed in triplicate, where the error bars correspond to the S.D. The observed IC_{50} values were used to calculate the K_i values according to Eq. (1). The apparent EC_{50}, K_i, and n_H values were summarized in Table 2.

Table 2
Binding affinity of varenicline for different binding sites at various nAChR subtypes.

nAChR subtype	Radioligand	K_i [a]	n_H [b]	Apparent EC_{50} [c]	n_H [b]
hα4β2	[^{3}H]Cytisine	90 ± 7 pM	1.00 ± 0.07	–	–
	[^{3}H]Imipramine [f]	~12 mM	0.46 ± 0.15	–	–
hα4β4	[^{3}H]Cytisine	121 ± 4 pM	1.11 ± 0.03	–	–
hα3β4	[^{3}H]Epibatidine	13 ± 1 nM	1.26 ± 0.10	–	–
hα7	[^{3}H]MLA	77 ± 6 nM	1.15 ± 0.10	–	–
Torpedo	[^{3}H]Cytisine	116 ± 8 μM [d]	1.21 ± 0.14	1.1 ± 0.2 μM	1.36 ± 0.33
	[^{3}H]TCP	No binding [e]	–	1.4 ± 0.2 μM	1.10 ± 0.12

[a] K_i values were calculated from Fig. 2A ([^{3}H]cytisine experiments), Fig. 2B ([^{3}H]MLA experiments), Fig. 2C ([^{3}H]epibatidine experiments), and Fig. 3A ([^{3}H]TCP experiments), respectively, according to Eq. (1).
[b] Hill coefficients.
[c] These values were obtained in the absence of any ligand (receptors are in the resting but activatable state).
[d] This value was obtained in the presence of proadifen (receptors are mainly in the desensitized state).
[e] This result was obtained in the presence of CCh (receptors are mainly in the desensitized state).
[f] These apparent IC_{50} and apparent n_H values were obtained from Fig. 3B.

The results obtained for hα4β2 nAChR suggest that varenicline interacts with the ORT sites (Fig. 4B) and three A binding sites (i.e., A1–3). A1 is located within the α4 subunit (Fig. 4C), whereas A2 and A3 are located at the inner (Fig. 4D) and outer surface, respectively, formed between the α4- and β2-EXDs. Although the interaction of varenicline with the A3 site was considered stable (see Fig. S1D; Supporting information), this interaction becomes unstable when varenicline also interacts with the ORT sites (see Fig. S2D; Supporting information), and consequently, this site is not included in Fig. 4 and Table 3.

At the ORT site, the aromatic portion of varenicline is stabilized by hydrophobic interactions with the aromatic cage formed by residues from the principal component (i.e., α4-Tyr98, α4-Tyr-202, α4-Tyr195, and α4-Trp154) (Fig. 4B; Table 3). Moreover, varenicline interacts with Loop C (i.e., Cys197–Cys198), two polar residues (i.e., α4-Ser153 and α4-Thr155) and several residues from the complementary component (i.e., β2-Leu121 and β2-Asn109). Two hydrogen bonds are additionally formed, one between the piperidine nitrogen of the ligand and the hydroxyl group of α4-Tyr98, and another between the same nitrogen and the carbonyl from the β2-Trp154 backbone. In A1, varenicline is stabilized within the α4 subunit through van der Waals interactions with Leu40, Ile42, Leu45, Met55, Val59, Tyr129, Met149, Phe151, Tyr207, and Phe209 (Fig. 4C; Table 3). In addition, varenicline forms one hydrogen bond between its pyrazine nitrogen and the carbonyl from the Cys147 backbone. In A2, varenicline is stabilized by van der Waals contacts with α4-Ile95, α4-Val96, α4-Leu97, α4-Pher105, α4-Gly103, β2-Val104, β2-Phe106, and β2-Tyr107 (Fig. 4D; Table 3). The aromatic portion of varenicline may act as hydrogen bond acceptor, whereas β2-Thr155 (ORT site), Thr57 (A1 site), and Tyr107 and a water molecule (A2 site), may serve as hydrogen bond donors. Furthermore, an electrostatic interaction is formed between the positively charged pyrazine nitrogen of varenicline and the negatively charged amino moiety of α4-Asp104 (A2 site). Three additional water-mediated hydrogen bonds are formed with the carbonyl from the α4-Gly103 and α4-Asp104 backbones as well as with the hydroxyl group of β2-Ser105 (A2 site) (Fig. 4D). Another water molecule is present in A2, forming an internal network of hydrogen bonds that stabilizes the ligand in this binding pocket.

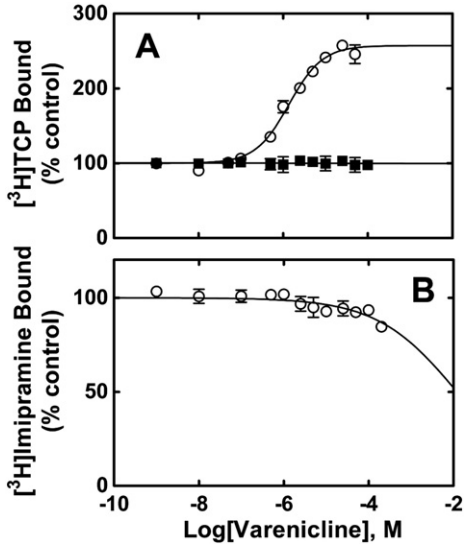

Fig. 3. Modulation of (A) [^{3}H]TCP binding to *Torpedo* nAChRs and of (B) [^{3}H]imipramine binding to hα4β2 nAChRs by varenicline. AChR membranes were pre-incubated (20 min) with 20 nM [^{3}H]TCP or 13 nM [^{3}H]imipramine, in the presence of 1 mM CCh (*Torpedo* nAChRs are mainly in the desensitized state) (■) or in the absence of any ligand (nAChRs are in the resting but activatable state) (○), and then equilibrated with increasing concentrations of varenicline. Nonspecific binding was determined at 1 mM CCh (A) or 100 μM imipramine (B). Each plot is the combination of two separated experiments each one performed in triplicate, where the error bars correspond to the S.D. The observed IC_{50} values were used to calculate the K_i values according to Eq. (1). The apparent EC_{50}, K_i, and n_H values were summarized in Table 2.

In the hα4β4 nAChR, varenicline interacts only with the ORT site (Fig. 5A; Table 3). The ligand is stabilized by hydrophobic interactions with aromatic residues from the principal component as well as nonpolar residues from the complementary component as suggested for the hα4β2 nAChR, as well as with β4-Ile113. Moreover, three hydrogen bonds are formed, two between the piperidine nitrogen of the ligand and the hydroxyl group of α4-Tyr98 or the carbonyl from the α4-Trp154 backbone, and the third between the pyrazine nitrogen of the molecule and the indole nitrogen of α4-Trp154. In addition, the aromatic portion of varenicline acts as a hydrogen bond acceptor, whereas β2-Tyr202 serves as a hydrogen bond donor.

Regarding the hα3β4 nAChR, varenicline interacts with the ORT and A2 sites (Table 3). In the ORT site, varenicline interacts with practically the same residues proposed for the hα4β2 and hα4β4 nAChRs (Table 3). In addition, two hydrogen bonds are formed with α3-Tyr93 and α3-Trp149, respectively (data not shown). In A2, varenicline interacts by van der Waals contacts with nonpolar residues as suggested for hα4β2 nAChR (Fig. 4B; Table 3). In addition, its pyrazine nitrogen forms a hydrogen bond with the carbonyl from the α3-Phe100 backbone (data not shown).

Regarding the hα7 nAChR, varenicline interacts with the ORT site (Fig. 5B) as well as with an additional allosteric site (i.e., A4), located at the complementary component (Fig. 5C). In the ORT site, varenicline is stabilized by hydrophobic interactions with aromatic residues (Fig. 5B; Table 3) as suggested for the hα4β2 nAChR. Moreover, the ligand interacts with residues from Loop C (i.e., Cys190) and the complementary component (i.e., Asn107, Gln117, Leu119, and Ser150), and a hydrogen bond is formed between the piperidine nitrogen of the ligand

Table 3
Residues involved in the binding of protonated varenicline at the orthosteric and allosteric (A) binding sites from the hα7, hα4β4, hα4β2, and hα3β4 nAChR models.

nAChR subtype	Orthosteric site	A1 site	A2 site	A4 site
hα4β2	α4-C197	α4-S131	α4-I95	
	α4-C198	α4-Y207	α4-V96	
	α4-Y195	α4-A208	α4-L97	
	α4-Y202	α4-C147	α4-G103	
	α4-Y98	α4-T148	α4-D104	
	α4-W154	α4-F209	α4-F105	
	α4-S153	α4-M149	β2-V104	
	α4-T155	α4-L40	β2-S105	
	β2-N109	α4-I42	β2-F106	
	β2-L121	α4-V59	β2-Y107	
		α4-F151		
		α4-T57		
		α4-Y129		
		α4-M55		
hα4β4	α4-C197			
	α4-C198			
	α4-Y195			
	α4-Y202			
	α4-Y98			
	α4-W154			
	α4-T155			
	β4-N111			
	β4-I113			
	β4-L123			
hα7	α7-C190 (P)			α7-F33
	α7-Y188 (P)			α7-I54
	α7-Y195 (P)			α7-L56
	α7-Y93 (P)			α7-M58
	α7-W149 (P)			α7-K87
	α7-W55 (C)			α7-P88
	α7-N107 (C)			α7-I90
	α7-Q117 (C)			α7-F100
	α7-L119 (C)			α7-P120
	α7-S150 (C)			α7-P121
				α7-G122
				α7-F146
hα3β4	α3-Y93		α3-V91	
	α3-Y190		α3-L92	
	α3-Y197		α3-F124	
	α3-C192		α3-A96	
	α3-C193		α3-F100	
	α3-W149		β4-Y109	
	β4-L112		β4-V106	
	β4-I113		β4-V108	
	β4-L123			
	β4-S150			
	β4-N111			

P, principal component; C, complementary component.

and the hydroxyl group of Trp149. In A4, varenicline is stabilized by a hydrogen bond formed between its piperidine nitrogen and the carbonyl from the Pro120 backbone (Fig. 5C). The ligand also interacts with nonpolar as well as ionized residues (Table 3), whereas its aromatic portion acts as a hydrogen bond acceptor interacting with the hydrogen bond donor Phe100 (Fig. 5C).

3.4. Molecular dynamics simulations

The MD simulations of varenicline docked to each binding site from each studied nAChRs subtype indicated that the complexes are stable during the 15-ns simulations (Fig. S1A–E; Supporting information). The calculated root mean square deviation (RMSD) values for each suggested site (Table 3) are below 0.5 Å, supporting the view that the observed interactions (Figs. 4 and 5) are stable. Furthermore, the potential energy value for each stable interaction was calculated from the MD simulations (Figs. S1F and S2E; Supporting information). The results indicating that the potential energy values are constant support the quality of the performed MD simulations and that they can be used to measure the distance between the amino acids involved in the capping of Loop C.

Additional MD simulations, performed when varenicline is bound to each allosteric site while the ORT sites are also occupied, indicate that the interaction with A1 (Fig. S2B) or A2 (Fig. S2C) is stable, whereas the interaction with A3 is unstable (Fig. S2D) (see Supporting information). To determine how the binding of varenicline to A1 or A2 modifies the capping of Loop C, the average distance between the hydroxyl group of α4-Tyr195 (Loop C) and the amino group of α4-Lys150 (β7 strand) as well as the average distance between the amino group of α4-Lys150 and the carboxyl group of α4-Asp204 (β10 strand) were first calculated when varenicline interacts with only the ORT sites and then contrasted to that when the A1 or A2 site is also occupied. Under these conditions, our results indicate that the distance between α4-Tyr195 and α4-Lys150 is increased, whereas the distance between α4-Lys150 and α4-Asp204 is decreased (Table 4). When varenicline interacts with the ORT and any of the allosteric sites, the average distance between the carboxyl group of α4-Glu200 (Loop C) and the amino group of β2-Lys79 (β1–β2 loop) was also increased and subsequently the corresponding salt bridge is broken, whereas the average distance required for the stable hydrogen bond between the backbone N–H of α4-Lys158 and the backbone carbonyl of α4-Ile201 was not affected (Fig. 6A; Table 4). In conclusion, the interaction of varenicline to A1 or A2 modifies the capping of Loop C, compared to that in which none of the allosteric sites is occupied (Fig. 6).

4. Discussion

As part of our attempt to characterize the interaction of varenicline with several nAChRs as well as to define why this ligand behaves as a full or partial agonist depending on the studied nAChR subtype, functional and structural approaches were used.

Our Ca^{2+} influx results indicate that varenicline activates nAChRs with the following rank sequence (EC_{50}s in μM): hα7 (0.18 ± 0.02) > hα4β4 (0.37 ± 0.08) > hα4β2 (1.30 ± 0.18) > hα3β4 (6.4 ± 1.2) ≫ > hα1β1γδ (>100). Based on the observed efficacy (E_{max}), varenicline behaves as a full agonist of hα7 and hα4β4 nAChRs, and as a partial agonist of hα4β2 and hα3β4 nAChRs. This is the first report showing that varenicline behaves as a full agonist of hα4β4 nAChRs. Different intrinsic properties and functional roles have been described for the α4β4 and α4β2 nAChRs. For instance, α4β4 nAChRs showed higher agonist potencies and slower desensitization [45,46] as well as lower propensity to nicotine-induced upregulation [47] compared to that for α4β2 nAChRs. Subsequently, hα4β4 nAChRs might still maintain cholinergic function after chronic exposure of nicotine concentrations found during smoking (i.e., ~0.3 μM). In addition, knockout mice studies demonstrated that β2-containing nAChRs are implicated in the reinforcing properties of nicotine [6] whereas β4-containing nAChRs play important roles in nicotine withdrawal symptoms [48]. Finally, individuals with the β4 subunit mutations (e.g., Arg136Trp and Met467Val) have higher sensitivity to ACh [49], and subsequently, they could be more sensitive to the addictive activity of nicotine. This evidence points out important differences between α4β2 and α4β4 nAChRs, and suggests that α4β4 AChRs could also be involved in the clinical activity of varenicline.

Combining our and previous [12] radioligand binding results, the following receptor selectivity for varenicline is obtained: hα4β2 (90 ± 7 pM) > hα4β4 (121 ± 4 pM) > hα3β4 (13 ± 1 nM) > hα7 (77 ± 6 nM) > hα4α6β4 AChR (110 ± 13 nM; [12]) ≫ > Tα1β1γδ (116 ± 8 μM). Based on previous studies, the subunit α6 seems to decrease the varenicline binding affinity [12,44]. Based on the molecular docking and MD results, we propose that the higher affinity of varenicline for the hα4β4 and hα4β2 nAChRs compared to that for the hα7, hα3β4, and *Torpedo* nAChRs may be ascribed to the observed higher number of hydrogen bonds at α4-containing AChRs compared to other nAChR subtypes.

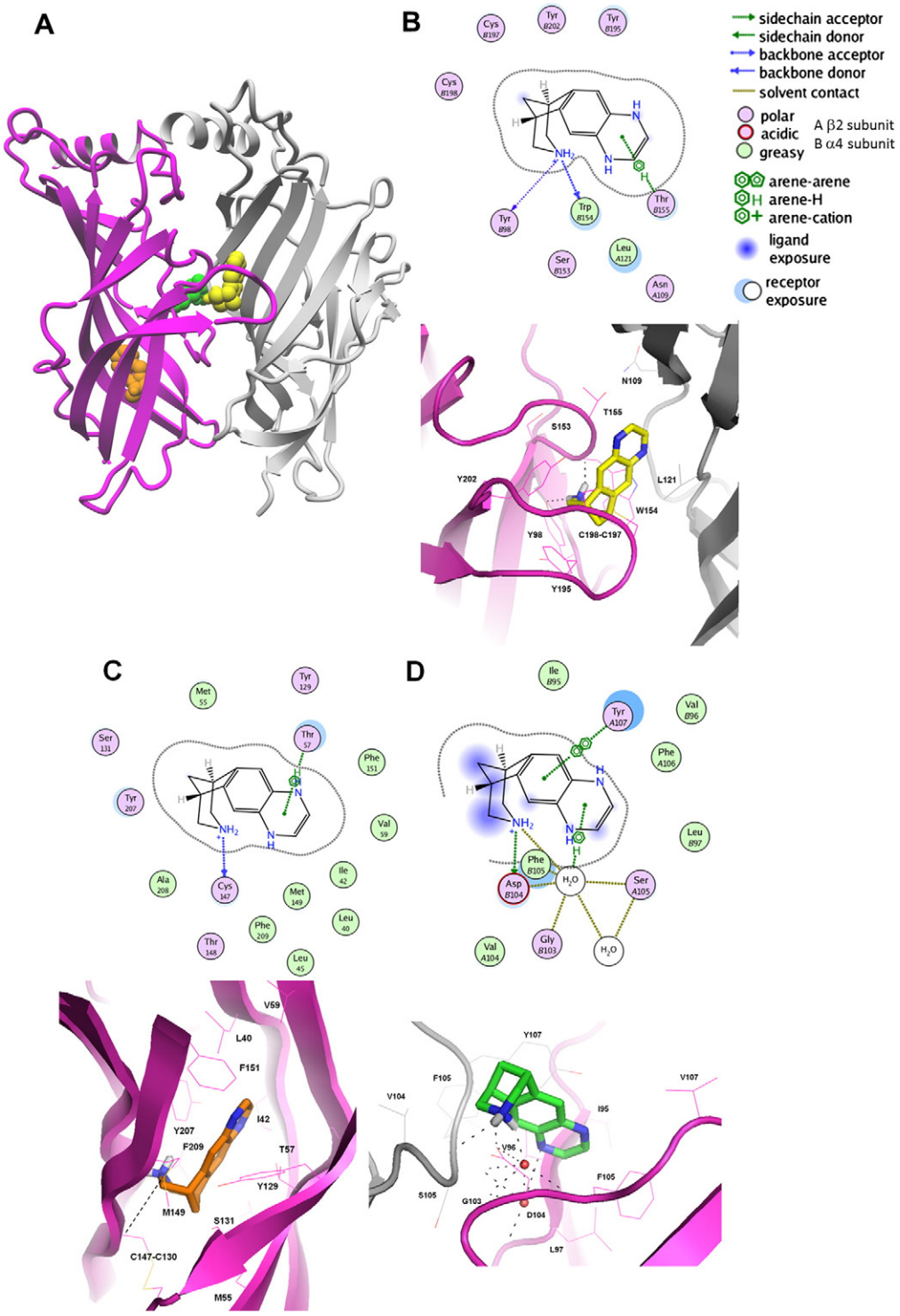

Fig. 4. Docking of protonated varenicline to the extracellular domain of the hα4β2 nAChR model. (A) Side view of the orthosteric (ORT) and allosteric (A) sites for varenicline (yellow) at the hα4β2 nAChR. The A1 site is located within the α4 subunit (orange), whereas the A2 site (green) is located at the inner surface formed between the α4- and β2-EXDs. (B) 3D and 2D (scheme) views of varenicline (yellow) interacting with the ORT site. The aromatic portion of the ligand is stabilized by hydrophobic interactions with the aromatic cage formed by residues from the principal component (i.e., α4-Tyr98, α4-Tyr-202, α4-Tyr195, and α4-Trp-154). Varenicline also interacts with Loop C (i.e., Cys197–Cys198), two polar residues (i.e., α4-Ser153 and α4-Thr155) and several residues from the complementary component (i.e., β2-Leu121 and β2-Asn109). Moreover, two hydrogen bonds are formed, one between the piperidine nitrogen of the ligand and the hydroxyl group of α4-Tyr98, and another with the carbonyl from the α4-Trp154 backbone. (C) 3D and 2D (scheme) views of varenicline (orange) interacting with the A1 site, located within the α4 subunit. The molecule is stabilized by van der Waals interactions with Leu40, Ile42, Met55, Val59, Tyr129, Met149, Phe151, Tyr207, and Phe209. In addition, varenicline forms a hydrogen bond between its pyrazine nitrogen and the carbonyl from the Cys147 backbone. (D) 3D and 2D (scheme) views of varenicline (green) interacting with the A2 site, located at the inner surface of the α4-/β2-EXD interface. The ligand is stabilized by van der Waals contacts with α4-Ile95, α4-Val96, α4-Leu97, α4-Gly103, β2-Val104, α4-Pher105, β2-Phe106, and β2-Tyr107. In addition, an electrostatic interaction is formed between its positively charged pyrazine nitrogen and the negatively charged amino moiety of α4-Asp104. Three additional water-mediated hydrogen bonds are formed, two with the carbonyls from the α4-Gly103 and α4-Asp104 backbone, and another with the hydroxyl group of β2-Ser105. Another water molecule in A2 forms an internal network of hydrogen bonds that stabilizes the ligand. For clarity, one α4 and two β2 subunits are hidden, whereas the other α4 and β2 subunits are shown in magenta and gray, respectively. The ligand is rendered in ball (A) or stick (B–E) mode. The residues involved in ligand binding are presented in 2D or shown explicitly in stick mode and are colored in red or gray, depending on the subunit. The nonpolar hydrogen atoms are hidden. When interactions occur within one receptor subunit, chain labels are not shown.

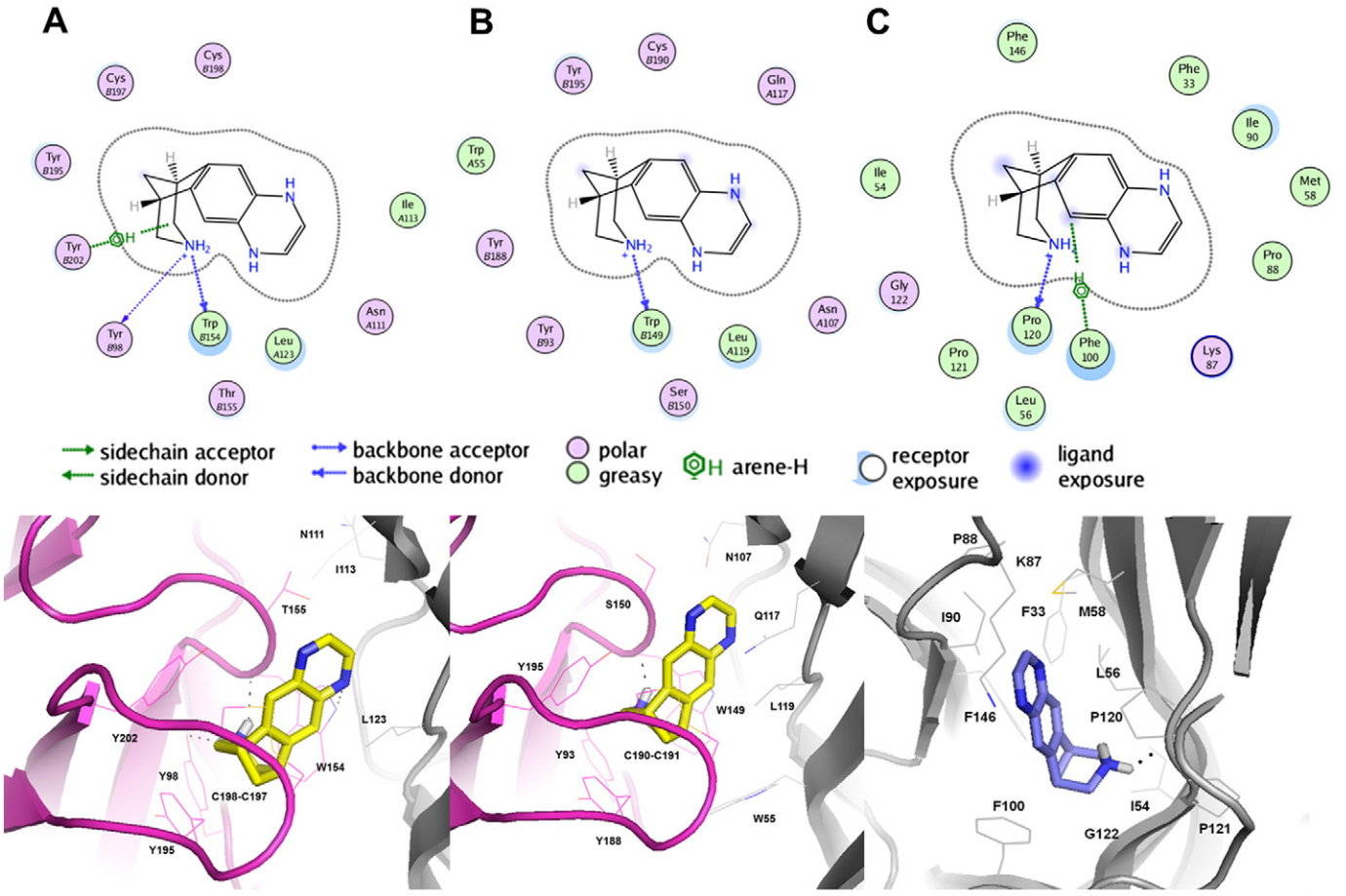

Fig. 5. Docking results of protonated varenicline to the extracellular domain of the hα4β4 and hα7 nAChR models. (A) 3D and 2D (scheme) views of varenicline (yellow) interacting with the ORT site at the hα4β4 nAChR. The ligand is stabilized by hydrophobic interactions with the aromatic cage formed by the same residues from the principal component as suggested for the hα4β2 nAChR (see Fig. 4). Three hydrogen bonds are formed, two between the piperidine nitrogen of the ligand and either the hydroxyl group of α4-Tyr98 or the carbonyl from the α4-Trp154 backbone, and another between the pyrazine nitrogen of the molecule and the indole nitrogen of α4-Trp154. Moreover, varenicline interacts with the same residues from Loop C as well as nonpolar residues (i.e., β4-N111, β4-Ile113, and β4-Leu123) that were suggested for the hα4β2 nAChR (see Fig. 4). (B) Detailed view and scheme interactions of varenicline (yellow) binding to the ORT site at the hα7 nAChR. In this site, the ligand is stabilized by hydrophobic interactions with aromatic residues from the principal (i.e., Tyr93, Tyr188, Tyr195, and Trp149) and complementary (i.e., Trp55) components. In addition, the ligand interacts with residues from Loop C (i.e., Cys190), and from the complementary component (i.e., Asn107, Gln117, Leu119, and Ser150), and a hydrogen bond is formed between the piperidine nitrogen of the ligand and the hydroxyl group of Trp149. (C) Detailed view and scheme interactions of varenicline (purple) at the A4 site, located within the α7 subunit. In this site, varenicline is stabilized by a hydrogen bond formed between its piperidine nitrogen and the carbonyl from the Pro120 backbone. In addition, the molecule interacts with nonpolar (i.e., Phe33, Ile54, Leu56, Met58, Pro88, Ile90, Phe100, Pro120, Pro121, Gly122, and Phe146) as well as ionized (i.e., Lys87) residues, whereas its aromatic portion acts as a hydrogen bond acceptor where Phe100 serves the hydrogen bond donor. For clarity, the principal and complementary components at the hα4β4 and hα7 nAChR-EXDs are shown in magenta and gray, respectively. The ligand is rendered in stick mode. The residues involved in ligand binding are presented in 2D or shown explicitly in stick mode, and colored in red or gray, depending on the subunit. The nonpolar hydrogen atoms are hidden.

The Ca^{2+} influx results also indicate that varenicline is more potent as an antagonist (nM concentration range) than as an agonist (μM concentration range). However, differences among nAChR subtypes are observed: the EC_{50}/IC_{50} ratio for the hα4β2 is the highest (464) compared to that for the hα4β4 (14), hα7 (2.6), and hα3β4 (2.7) nAChRs. Further experimental evidence is needed to understand these unexpected findings. The Ca^{2+} results are in agreement with the experimental evidence indicating that varenicline (1 mg twice-daily) activates only minimal fractions of α3β4 and α4β2 (<2%), and α7 (<0.05%) AChRs, whereas it inhibits these receptors in a selective manner: α4β2 (42%–56%) > α7 (16%) > α3β4 (11%) [50]. The 10-fold higher antagonistic potency of varenicline for the hα4β2 compared to that for the hα4β4 nAChR can be explained by its higher desensitizing activity at the hα4β2 nAChR [45]. Moreover, the functional effects of therapeutic varenicline concentrations at α7 nAChRs are not related to α7 nAChR activation but to desensitization of moderate fractions of this subtype [50].

Table 4
Average distance between residues involved in varenicline interaction to the hα4β2 nAChR when the agonist binds only to the orthosteric sites compared to that when it binds to both the orthosteric site and the respective A1 or A2 allosteric site.

Interactive residues	Interaction type	Average distance [Å]		
		Orthosteric site (only)	Orthosteric and A1 sites	Orthosteric and A2 sites
α4-Tyr195/α4-Lys150	Hydrogen bond	6.00	8.83	7.80
α4-Lys150/α4-Asp204	Salt bridge	8.03	6.09	7.04
α4-Glu200/β2-Lys79	Salt bridge	4.08	6.37	9.47
α4-Lys158/β2-Ile201	Hydrogen bond	1.97	2.07	2.10

Our radioligand results indicate that varenicline enhances [^{3}H]cytisine and [^{3}H]TCP binding to *Torpedo* nAChRs in the resting but activatable state, consistent with the idea that varenicline induces nAChR desensitization, but ruling out the possibility of AChR ion channel blocking by binding to the TCP/imipramine site located in the middle of the ion channel [52]. Our molecular docking and MD simulation results support the possibility that varenicline modulates α4β2 and α3β4 nAChRs by binding to allosteric sites similar to that reported for the partial agonist (−)-cytisine [51]. Since (−)-cytisine also binds to a homologous A1 site at *Torpedo* nAChRs [51], we suggest that these extracellular allosteric binding sites are part of a novel mechanism underlying partial agonism at selective AChRs.

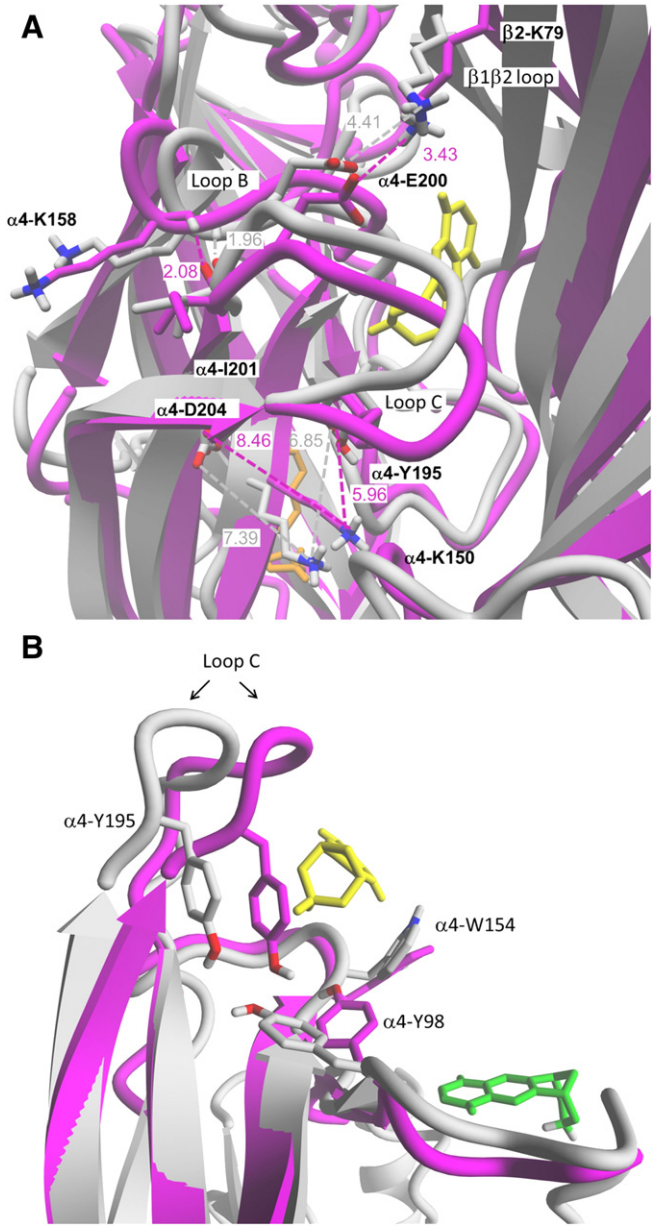

Fig. 6. Capping of Loop C induced by varenicline binding to the allosteric A1 (A) or A2 (B) site when the orthosteric (ORT) sites at the hα4β2 nAChR are also occupied compared to that when the agonist binds only to the ORT sites. (A) The MD results show an increased distance between the hydroxyl moiety of α4-Tyr195 (Loop C) and the amino moiety of α4-Lys150 (β7 strand), and concomitantly a decreased distance between the amino moiety of α4-Lys150 and the carboxyl group of α4-Asp204 (β10 strand). On the other hand, a stable hydrogen bond interaction between the carboxyl group of α4-Lys158 (Loop B) and the carbonyl group from the α4-Ile201 (Loop C) backbone is observed, whereas the salt bridge between the carboxyl group of α4-Glu200 (Loop C) and the amino moiety of β2-Lys79 (β1-β2 loop) is broken when varenicline interacts with the A1 site (orange) while the ORT sites are also occupied (yellow). The calculated average distances between residues are summarized in Table 4. (B) The MD results show a wider gap between the Loop C and the surface of the adjacent β2 subunit, indicating a decreased capping of Loop C when varenicline binds to A2 (green) while the ORT sites are also occupied (yellow). Similar results were obtained for A1. For a better visualization, the α4 subunit is rotated 90° compared to that in (A). Varenicline and the most important residues are presented in stick mode, whereas the nonpolar hydrogen atoms are hidden. The nAChR subunits are shown in magenta when varenicline binds only to the ORT sites, whereas they are in gray when the agonist also interacts with the allosteric site.

When agonists bind to AChBPs and nAChRs, the capping of Loop C draws a conserved Tyr185 (corresponding to α4-Tyr195 from Loop C) into register with a conserved Lys139 (corresponding to α4-Lys150 from β7 strand), forming a hydrogen bond or possibly a salt bridge, and subsequently decreasing the distance between these two residues [53]. In this regard, the calculated distances for nicotine and CCh, two full agonists, are in the range of 2–3 Å [54]. These changes also weaken the electrostatic link between Lys139 and Asp194 [corresponding to α4-Lys150 (β7 strand) and α4-Asp204 (β10 strand), respectively]. Interestingly, the capping of Loop C produced by partial agonists is in-between the movements elicited by full agonists (i.e., Loop C is in closed conformation) and that in the absence of ligands (i.e., Apo state), when Loop C is in the open conformation [55–57]. When varenicline binds to the ORT sites, the concomitant movement of Loop C (i.e., intermediate capping) produced a distance of 6.00 Å between α4-Tyr195 and α4-Lys150. Our results with varenicline using the hα4β2 nAChR model are in agreement with previous measurements (6.85 Å) at the AChBP [30]. These results support the notion that this ligand is a partial agonist of both hα4β2 and hα3β4 nAChRs. As an alternative explanation, this partial agonism might be attributed to the interaction of varenicline with the allosteric sites observed at these receptor subtypes. In this regard, we tested the hypothesis that when varenicline binds to either A1 or A2 site at the hα4β2 nAChR it induces conformational changes at Loop C, limiting the course of capping, the first step in the gating process [56,57]. The results show an increase in the average distance between α4-Tyr195 and α4-Lys150 and a concomitant decrease in the average distance between α4-Asp204 and α4-Lys150 when varenicline is bound to either A1 or A2 site, compared to that in the absence of allosteric site occupancy. In this regard, the observed increased distance elicited by varenicline (7.80–8.83 Å), which is close to that in the Apo state (8.5 Å) [30] suggests a decreased capping of Loop C, impairing the first step in the process of nAChR gating.

The electrostatic interactions involving negatively charged residues at the β1–β2 loop are important for intersubunit contacts, whereas several of its residues are essential for gating [58]. In our study, a stable salt bridge was observed between α4-Glu200 (Loop C) and β2-Lys79 (β1–β2 loop) when varenicline interacts only with the ORT sites. The distance between these two residues (4.08 Å) was increased (6.37–9.47 Å) when varenicline also interacts with each allosteric site. In this regard, when varenicline binds to any of the allosteric sites, it weakens this salt bridge, limiting the capping of Loop C at the hα4β2 nAChR. The same mechanism was observed for halothane at the hα4β2 nAChR, although this general anesthetic interacts with an allosteric locus near the agonist site but differs from the A1 or A2 site [59]. This suggests that varenicline, in addition to be an agonist, has negative allosteric modulatory properties at hα4β2 and hα3β4 nAChRs. On the other hand, the hydrogen bonds and salt bridges in the region formed between Loop C residues and Lys158, a critical residue from Loop B involved in nicotine affinity [54] was not altered when varenicline interacts with the allosteric sites, ruling out the possibility that this interaction decreases the affinity for these receptors.

The allosteric sites A1 and A2 have not been found in all studied nAChR subtypes. At the hα4β2 nAChR, the A1 site is formed only by α4 subunit residues (i.e., intrasubunit site), whereas no A1 site was found at the hα4β4 nAChR (see Table 3). The A2 site at the hα4β2 nAChR is formed by several α4 and β2 residues (i.e., intersubunit site), whereas at the hα3β4 nAChR, this site is formed by several α3 residues but only one β4 residue (Y104) (the sequence similarity between the β2 and β4 subunits is ~60%). Since the A1 site at the hα4β2 nAChR is formed only by α4 residues, the allosteric effect of the β4 subunit from the hα4β4 nAChR might be precluding the formation of the intrasubunit pocket within the α4 subunit. We tested whether the β4 subunit changes the shape (e.g., by decreasing the volume) and properties (e.g., by preventing the formation of the hydrogen bonds network) of the varenicline binding pocket as seen in the hα4β2 nAChR, and the differences are too small to confirm this possibility. An alternative possibility is a difference in the varenicline access route to reach its pocket between both AChRs. However, to test this hypothesis would require far

more demeaning MD simulations and other modeling studies that are beyond the scope of this manuscript.

Based on our work, we propose that hα4β4 nAChRs are also potential targets for the clinical activity of varenicline. From the molecular point of view, the observed higher number of hydrogen bonds at α4-containing nAChRs may explain the higher affinity of varenicline for the hα4β4 and hα4β2 nAChRs compared to that for other receptor subtypes. Although varenicline can activate hα4β2 and hα3β4 nAChRs by binding to the ORT sites, its interaction with either allosteric site may limit the first step in the gating process, contributing to the observed partial agonistic activity at these nAChR subtypes.

Acknowledgement

This work was partially supported by grants from the TEAM research subsidy from the Foundation for Polish Science (to K.J.), and from the National Science Center, Poland (SONATA funding, UMO-2013/09/D/NZ7/04549) [to K.T-D. (PI) and H.R.A. (Co-PI)]. The molecular modeling experiments were developed using the equipment purchased within the project "The equipment of innovative laboratories doing research on new medicines used in the therapy of civilization and neoplastic diseases" within the Operational Program Development of Eastern Poland 2007–2013, Priority Axis I modern Economy, operations I.3 Innovation promotion (to K.J. and A.K.). The research was partially performed during the postdoctoral Marie Curie fellowship of Dr. Kaczor at University of Eastern Finland, Kuopio, Finland, and during the scholar visit of Dr. Targowska-Duda at this University. Calculations were partially performed under a computational grant by the Interdisciplinary Center for Mathematical and Computational Modeling (ICM), Warsaw, Poland (grant number G30-18, to A.K.) and under resources and licenses from CSC, Finland (to A.K. and A.P.). The authors thank to National Institute on Drug Addiction (NIDA, NIH, Bethesda, Maryland, USA) for its gift of varenicline hydrochloride and phencyclidine hydrochloride.

Appendix A. Supplementary data

Supplementary data to this article can be found online at http://dx.doi.org/10.1016/j.bbamem.2014.11.003.

References

[1] M. Nides, E.D. Glover, V.I. Reus, A.G. Christen, B.J. Make, C.B. Billing Jr., K.E. Williams, Varenicline versus bupropion SR or placebo for smoking cessation: a pooled analysis, Am. J. Health Behav. 32 (2008) 664–675.
[2] H.R. Arias, Is the inhibition of nicotinic acetylcholine receptors by bupropion involved in its clinical actions? Int. J. Biochem. Cell Biol. 41 (2009) 2098–2108.
[3] M.O. Ortells, H.R. Arias, Neuronal networks of nicotine addiction, Int. J. Biochem. Cell Biol. 42 (2010) 1931–1935.
[4] H. Rollema, J.W. Coe, L.K. Chambers, R.S. Hurst, S.M. Stahl, K.E. Williams, Rationale, pharmacology and clinical efficacy of partial agonists of α4β2 nACh receptors for smoking cessation, Trends Pharmacol. Sci. 28 (2007) 316–325.
[5] J.W. Smith, A. Mogg, E. Tafi, E. Peacey, I.A. Pullar, P. Szekeres, M. Tricklebank, Ligands selective for α4β2 but not α3β4 or α7 nicotinic receptors generalise to the nicotine discriminative stimulus in the rat, Psychopharmacology (Berl) 190 (2007) 157–170.
[6] M.R. Picciotto, M. Zoli, R. Rimondini, C. Lena, L.M. Marubio, E.M. Pich, K. Fuxe, J.P. Changeux, Acetylcholine receptors containing the β2 subunit are involved in the reinforcing properties of nicotine, Nature 391 (1998) 173–177.
[7] M. Shoaib, J. Gommans, A. Morley, I.P. Stolerman, R. Grailhe, J.P. Changeux, The role of nicotinic receptor β2 subunits in nicotine discrimination and conditioned taste aversion, Neuropharmacology 42 (2002) 530–539.
[8] S.R. Grady, N.M. Meinerz, J. Cao, A.M. Reynolds, M.R. Picciotto, J.P. Changeux, J.M. McIntosh, M.J. Marks, A.C. Collins, Nicotinic agonists stimulate acetylcholine release from mouse interpeduncular nucleus: a function mediated by a different nAChR than dopamine release from striatum, J. Neurochem. 76 (2001) 258–268.
[9] J.W. Coe, P.R. Brooks, M.G. Vetelino, M.C. Wirtz, E.P. Arnold, J. Huang, S.B. Sands, T.I. Davis, L.A. Lebel, C.B. Fox, A. Shrikhande, J.H. Heym, E. Schaeffer, H. Rollema, Y. Lu, R.S. Mansbach, L.K. Chambers, C.C. Rovetti, D.W. Schulz, F.D. Tingley III, B.T. O'Neill, Varenicline: an α4β2 nicotinic receptor partial agonist for smoking cessation, J. Med. Chem. 48 (2005) 3474–3477.
[10] K.B. Mihalak, F.I. Carroll, C.W. Luetje, Varenicline is a partial agonist at α4β2 and a full agonist at α7 neuronal nicotinic receptors, Mol. Pharmacol. 7 (2006) 801–805.
[11] H. Rollema, L.K. Chambers, J.W. Coe, J. Glowa, R.S. Hurst, L.A. Lebel, Y. Lu, R.S. Mansbach, R.J. Mather, C.C. Rovetti, S.B. Sands, E. Schaeffer, D.W. Schulz, F.D. Tingley III, K.E. Williams, Pharmacological profile of the α4β2 nicotinic acetylcholine receptor partial agonist varenicline, an effective smoking cessation aid, Neuropharmacology 52 (2007) 985–994.
[12] H. Rollema, A. Shrikhande, K.M. Ward, F.D. Tingley III, J.W. Coe, B.T. O'Neill, E. Tseng, E.Q. Wang, R.J. Mather, R.S. Hurst, K.E. Williams, M. de Vries, T. Cremers, S. Bertrand, D. Bertrand, Pre-clinical properties of the α4β2 nicotinic acetylcholine receptor partial agonists varenicline, cytisine and dianicline translate to clinical efficacy for nicotine dependence, Br. J. Pharmacol. 160 (2010) 334–345.
[13] R.C. Jiloha, Pharmacotherapy of smoking cessation, Indian J. Psychiatry 5 (2014) 87–95.
[14] E.C. O'Connor, D. Parker, H. Rollema, A.N. Mead, The α4β2 nicotinic acetylcholine-receptor partial agonist varenicline inhibits both nicotine self-administration following repeated dosing and reinstatement of nicotine seeking in rats, Psychopharmacology (Berl) 208 (2010) 365–376.
[15] C. Reperant, S. Pons, E. Dufour, H. Rollema, A.M. Gardier, U. Maskos, Effect of the α4β2* nicotinic acetylcholine receptor partial agonist varenicline on dopamine release in β2 knock-out mice with selective re-expression of the β2 subunit in the ventral tegmental area, Neuropharmacology 58 (2010) 346–350.
[16] L. Azam, U.H. Winzer-Serhan, Y. Chen, F.M. Leslie, Expression of neuronal nicotinic acetylcholine receptor subunit mRNAs within midbrain dopamine neurons, J. Comp. Neurol. 444 (2002) 260–274.
[17] M. Quik, Y. Polonskaya, A. Gillespie, M. Jakowec, G.K. Lloyd, J.W. Langston, Localization of nicotinic receptor subunit mRNAs in monkey brain by in situ hybridization, J. Comp. Neurol. 425 (2000) 58–69.
[18] H.R. Arias, N.B. Fedorov, L.C. Benson, P. Lippiello, G.J. Gatto, D. Feuerbach, M.O. Ortells, Functional and structural interaction of (−)-reboxetine with the human α4β2 nicotinic acetylcholine receptor, J. Pharmacol. Exp. Ther. 344 (2013) 113–123.
[19] H.R. Arias, K.M. Targowska-Duda, K. Jozwiak, N,6-dimethyltricyclo[5.2.1.$0^{2,6}$]decan-2-amine enantiomers interact with the human α4β2 nicotinic acetylcholine receptor at luminal and non-luminal domains, OA Biochemistry 1 (2013) 11.
[20] H.R. Arias, D. Feuerbach, P. Bhumireddy, M.O. Ortells, Inhibitory mechanisms and binding site location for serotonin selective reuptake inhibitors on nicotinic acetylcholine receptors, Int. J. Biochem. Cell Biol. 42 (2010) 712–724.
[21] H.R. Arias, J.R. Trudell, E.Z. Bayer, B. Hester, E.A. McCardy, M.P. Blanton, Noncompetitive antagonist binding sites in the *Torpedo* nicotinic acetylcholine receptor ion channel. Structure–activity relationship studies using adamantane derivatives, Biochemistry 42 (2003) 7358–7370.
[22] H.R. Arias, H. Xing, K. Macdougall, M.P. Blanton, F. Soti, W.R. Kem, Interaction of benzylidene-anabaseine analogues with agonist and allosteric sites on muscle nicotinic acetylcholine receptors, Br. J. Pharmacol. 157 (2009) 320–330.
[23] H.R. Arias, D. Feuerbach, K.M. Targowska-Duda, M. Russell, K. Jozwiak, Interaction of selective serotonin reuptake inhibitors with neuronal nicotinic acetylcholine receptors, Biochemistry 49 (2010) 5734–5742.
[24] Y. Aracava, E.X. Albuquerque, Meproadifen enhances activation and desensitization of the acetylcholine receptor-ionic channel complex (AChR): single channel studies, FEBS Lett. 17 (1984) 267–274.
[25] Y. Cheng, W.H. Prusoff, Relationship between the inhibition constant (K_i) and the concentration of inhibitor which causes 50 percent inhibition (IC_{50}) of an enzymatic reaction, Biochem. Pharmacol. 22 (1973) 3099–3108.
[26] A.R. Davies, D.J. Hardick, I.S. Blagbrough, B.V. Potter, A.J. Wolstenholme, S. Wonnacott, Characterisation of the binding of [^{3}H]methyllycaconitine: a new radioligand for labelling α7-type neuronal nicotinic acetylcholine receptors, Neuropharmacology 38 (1999) 679–690.
[27] Y.E. Slater, L.M. Houlihan, P.D. Maskell, R. Exley, I. Bermudez, R.J. Lukas, A.C. Valdivia, B.K. Cassels, Halogenated cytisine derivatives as agonists at human neuronal nicotinic acetylcholine receptor subtypes, Neuropharmacology 44 (2003) 503–515.
[28] J. Zhang, J.H. Steinbach, Cytisine binds with similar affinity to nicotinic α4β2 receptors on the cell surface and in homogenates, Brain Res. 959 (2003) 98–102.
[29] S. Michelmore, K. Croskery, J. Nozulak, D. Hoyer, R. Longato, A. Weber, R. Bouhelal, D. Feuerbach, Study of the calcium dynamics of the human α4β2, α3β4 and α1β1γδ nicotinic acetylcholine receptors, Naunyn Schmiedeberg's Arch. Pharmacol. 366 (2002) 235–245.
[30] P. Rucktooa, C.A. Haseler, R. van Elk, A.B. Smit, T. Gallagher, T.K. Sixma, Structural characterization of binding mode of smoking cessation drugs to nicotinic acetylcholine receptors through study of ligand complexes with acetylcholine-binding protein, J. Biol. Chem. 28 (2012) 23283–23293.
[31] N. Unwin, Refined structure of the nicotinic acetylcholine receptor at 4 Å resolution, J. Mol. Biol. 346 (2005) 967–989.
[32] J.D. Thompson, D.G. Higgins, T.J. Gibson, CLUSTAL W: improving the sensitivity of progressive multiple sequence alignment through sequence weighting, position-specific gap penalties and weight matrix choice, Nucleic Acids Res. 22 (1994) 4673–4680.
[33] N. Eswar, B. Webb, M.A. Marti-Renom, M.S. Madhusudhan, D. Eramian, M.Y. Shen, U. Pieper, A. Sali, Comparative protein structure modeling using Modeller, Curr. Protoc. Bioinformatics, Supplement, 15, John Wiley & Sons, Inc., 2006 (5.6.1–5.6.30).
[34] M.Y. Shen, A. Sali, Statistical potential for assessment and prediction of protein structures, Protein Sci. 15 (2006) 2507–2524.
[35] F. Melo, E. Feytmans, Assessing protein structures with a non-local atomic interaction energy, J. Mol. Biol. 27 (1998) 1141–1152.
[36] J.U. Bowie, R. Luthy, D. Eisenberg, A method to identify protein sequences that fold into a known three-dimensional structure, Science 253 (1991) 164–170.

[37] R.A. Laskowski, M.W. MacArthur, D.S. Moss, J.M. Thornton, PROCHECK — a program to check the stereochemical quality of protein structures, J. Appl. Cryst. 26 (1993) 283–291.
[38] H.R. Arias, D. Feuerbach, K.M. Targowska-Duda, S. Aggarwal, D. Lapinsky, K. Jozwiak, Structural and functional interaction of (±)-2-(N-tert-butylamino)-3′-iodo-4′-azidopropiophenone, a photoreactive bupropion derivative, with nicotinic acetylcholine receptors, Neurochem. Int. 61 (2012) 1433–1441.
[39] K.J. Bowers, E. Chow, H. Xu, R.O. Dror, M.P. Eastwood, B.A. Gregersen, J.L. Klepeis, I. Kolossváry, M.A. Moraes, F.D. Sacerdoti, J.K. Salmon, Y. Shan, D.E. Shaw, Scalable algorithms for molecular dynamics simulations on commodity clusters, Proceedings of the ACM/IEEE Conference on Supercomputing (SC06), November 11–17, 2006 (Tampa, Florida).
[40] H. Nury, F. Poitevin, C. Van Renterghem, J.P. Changeux, P.J. Corringer, M. Delarue, M. Baaden, One-microsecond molecular dynamics simulation of channel gating in a nicotinic receptor homologue, Proc. Natl. Acad. Sci. U. S. A. 10 (2010) 6275–6280.
[41] A.A. Kaczor, Z. Karczmarzyk, A. Fruzinski, K. Pihlaja, J. Sinkkonen, K. Wiinamaki, C. Kronbach, K. Unverferth, A. Poso, D. Matosiuk, Structural studies, homology modeling and molecular docking of novel non-competitive antagonists of GluK1/GluK2 receptors, Bioorg. Med. Chem. 22 (2014) 787–795.
[42] Y. Xiao, H. Fan, J.L. Musachio, Z.L. Wei, S.K. Chellappan, A.P. Kozikowski, K.J. Kellar, Sazetidine-A, a novel ligand that desensitizes α4β2 nicotinic acetylcholine receptors without activating them, Mol. Pharmacol. 70 (2006) 1454–1460.
[43] D. Rayes, M.J. De Rosa, S.M. Sine, C. Bouzat, Number and locations of agonist binding sites required to activate homomeric Cys-loop receptors, J. Neurosci. 29 (2009) 6022–6032.
[44] S.R. Grady, R.M. Drenan, S.R. Breining, D. Yohannes, C.R. Wageman, N.B. Fedorov, S. McKinney, P. Whiteaker, M. Bencherif, H.A. Lester, M.J. Marks, Structural differences determine the relative selectivity of nicotinic compounds for native α4β2*-, α6β2*-, α3β4*- and α7-nicotine acetylcholine receptors, Neuropharmacology 58 (2010) 1054–1066.
[45] J. Wu, Q. Liu, K. Yu, J. Hu, Y.P. Kuo, M. Segerberg, P.A. St John, R.J. Lukas, Roles of nicotinic acetylcholine receptor beta subunits in function of human α4-containing nicotinic receptors, J. Physiol. 576 (2006) 103–118.
[46] C.L. Gentry, L.H. Wilkins Jr., R.J. Lukas, Effects of prolonged nicotinic ligand exposure on function of heterologously expressed, human α4β2- and α4β4-nicotinic acetylcholine receptors, J. Pharmacol. Exp. Ther. 304 (2003) 206–216.
[47] Y. Xiao, K.J. Kellar, The comparative pharmacology and up-regulation of rat neuronal nicotinic receptor subtype binding sites stably expressed in transfected mammalian cells, J. Pharmacol. Exp. Ther. 310 (2004) 98–107.
[48] R. Salas, F. Pieri, M. De Biasi, Decreased signs of nicotine withdrawal in mice null for the β4 nicotinic acetylcholine receptor subunit, J. Neurosci. 24 (2004) 10035–10039.
[49] Y. Liang, R. Salas, L. Marubio, D. Bercovich, M. De Biasi, A.L. Beaudet, J.A. Dani, Functional polymorphisms in the human β4 subunit of nicotinic acetylcholine receptors, Neurogenetics 6 (2005) 37–44.
[50] H. Rollema, C. Russ, T.C. Lee, R.S. Hurst, D. Bertrand, Functional interactions of varenicline and nicotine with nAChR subtypes implicated in cardiovascular control, Nicotine Tob. Res. 1 (2014) 733–742.
[51] H.R. Arias, K.M. Targowska-Duda, D. Feuerbach, K. Jozwiak, Mecamylamine inhibits muscle nicotinic acetylcholine receptors by competitive and noncompetitive mechanisms, OA Biochemistry 1 (2013) 7.
[52] H.R. Arias, P. Bhumireddy, C. Bouzat, Molecular mechanisms and binding site locations for noncompetitive antagonists of nicotinic acetylcholine receptors, Int. J. Biochem. Cell Biol. 38 (2006) 1254–1276.
[53] S.M. Sine, A.G. Engel, Recent advances in Cys-loop receptor structure and function, Nature 440 (2006) 448–455.
[54] P.H. Celie, S.E. van Rossum-Fikkert, W.J. van Dijk, K. Brejc, A.B. Smit, T.K. Sixma, Nicotine and carbamylcholine binding to nicotinic acetylcholine receptors as studied in AChBP crystal structures, Neuron 41 (2004) 907–914.
[55] H.R. Arias, Positive and negative modulation of nicotinic receptors, Adv. Protein Chem. Struct. Biol. 80 (2010) 153–203.
[56] H.R. Arias, Molecular interactions between ligands and nicotinic acetylcholine receptors revealed by studies with acetylcholine binding proteins, J. Thermodynam. Cat. 3 (2012) 116.
[57] C. Shi, R. Yu, S. Shao, Y. Li, Partial activation of α7 nicotinic acetylcholine receptors: insights from molecular dynamics simulations, J. Mol. Model. 19 (2013) 871–878.
[58] C. Bouzat, F. Gumilar, G. Spitzmaul, H.L. Wang, D. Rayes, S.B. Hansen, P. Taylor, S.M. Sine, Coupling of agonist binding to channel gating in an ACh-binding protein linked to an ion channel, Nature 430 (2004) 896–900.
[59] L.T. Liu, D. Willenbring, Y. Xu, P. Tang, General anesthetic binding to neuronal α4β2 nicotinic acetylcholine receptor and its effects on global dynamics, J. Phys. Chem. B 113 (2009) 12581–12589.